



This is a repository copy of *Data-driven adaptive robust optimization for energy systems in ethylene plant under demand uncertainty*.

White Rose Research Online URL for this paper:

<https://eprints.whiterose.ac.uk/180872/>

Version: Accepted Version

Article:

Shen, F., Zhao, L., Wang, M. orcid.org/0000-0001-9752-270X et al. (2 more authors) (2022) Data-driven adaptive robust optimization for energy systems in ethylene plant under demand uncertainty. *Applied Energy*, 307. 118148. ISSN 0306-2619

<https://doi.org/10.1016/j.apenergy.2021.118148>

Article available under the terms of the CC-BY-NC-ND licence (<https://creativecommons.org/licenses/by-nc-nd/4.0/>).

Reuse

This article is distributed under the terms of the Creative Commons Attribution-NonCommercial-NoDerivs (CC BY-NC-ND) licence. This licence only allows you to download this work and share it with others as long as you credit the authors, but you can't change the article in any way or use it commercially. More information and the full terms of the licence here: <https://creativecommons.org/licenses/>

Takedown

If you consider content in White Rose Research Online to be in breach of UK law, please notify us by emailing eprints@whiterose.ac.uk including the URL of the record and the reason for the withdrawal request.



eprints@whiterose.ac.uk
<https://eprints.whiterose.ac.uk/>

Data-driven adaptive robust optimization for energy systems in ethylene plant under demand uncertainty

Feifei Shen ^a, Liang Zhao ^{a, b, *}, Meihong Wang ^c, Wenli Du ^{a, b}, Feng Qian ^{a, b, *}

^a Key Laboratory of Smart Manufacturing in Energy Chemical Process, Ministry of Education, East China University of Science and Technology, Shanghai 200237, China

^b Shanghai Institute of Intelligent Science and Technology, Tongji University, Shanghai 200092, China

^c Department of Chemical and Biological Engineering, The University of Sheffield, Sheffield S1 3JD, United Kingdom

Abstract: The operational optimization of energy systems is of great significance for improving the overall efficiency of industrial processes. Facing new challenges brought by widespread uncertainties, a data-driven adaptive robust industrial multi-type energy systems optimization framework was proposed by bridging robust optimization and machine learning methods in this paper. The industrial data were used to capture the demand uncertainty of the actual process. Hybrid models of units were first developed considering the operational characteristics, and the energy system optimization model was then formed as a mixed-integer nonlinear programming problem. The uncertain parameter set of process power demands was formed by the process models using historical data of a whole operating period. Afterward, the uncertainty set was constructed by applying the robust kernel density estimation method, which can reduce conservatism by considering the distributional information. By integrating the derived data-driven uncertainty set, a two-stage adaptive robust optimization model aiming at minimizing the weighted total energy consumption was developed. The multi-level robust optimization model was reformulated as a tractable single-level model by employing the affine decision rule. A case study on a plant-wide industrial energy system in the ethylene plant was performed, and the minimum optimal energy consumption was 25,350 kg/h, whose price of robustness was only 2.18%. The robust optimization results can guide the operational optimization of energy systems under uncertainty for the operators of the ethylene plant.

Key words: energy systems, industrial big data, machine learning, uncertainty, adaptive robust optimization

1. Introduction

Energy systems, which are used to transport and transfer multiple types of energy, are

* Corresponding author. E-mail address: lzha@ecust.edu.cn (L. Zhao), fqian@ecust.edu.cn (F. Qian).

fundamental parts of large-scale chemical industries. The modeling and optimization of an industrial energy system can help reduce energy consumption and carbon dioxide emissions [1], [2]. One typical energy system in ethylene manufacturing mainly includes boilers for super-high-pressure steam (SS) production, a waste heat recycle system providing SS, steam turbines to satisfy process mechanical power demands, cooling towers for water circulation, and some heat exchangers [3]. Given that the energy system accounts for a large proportion of the operational cost of ethylene plants, the modeling and optimization of the industrial energy system are vital for improving the whole plant efficiency.

The steam turbine network involving SS, high-pressure steam (HS), medium-pressure steam (MS), and low-pressure steam (LS) is a crucial part of the energy systems, and much work has been performed on its modelling and optimization [4],[5]. Li et al. [6] developed an industrial data based turbine model and a mixed-integer nonlinear programming (MINLP) model for real steam turbine network optimization. However, the effect of the operational conditions of steam condensers was ignored in these studies. Reducing the cooling water temperature decreases the pressure in the steam condenser, which then increases the efficiency of the corresponding steam turbine and the energy cost in the cooling water system [7],[8]. Considering this issue, a multi-type energy system model was developed to balance the energy consumption in the sub-systems, and a seasonal energy system optimization was performed [3].

Although the modeling and optimization of energy systems have made considerable progress, their applicability to actual industrial energy systems is limited. In the deterministic energy system optimization, only specific operational conditions have been examined. The derived optimal operating conditions may not always adapt an industrial plant because of the presence of many uncertainties, such as varying unit efficiencies and fluctuating process demands. Recent studies have focused on optimization under various uncertainties. Specific methods, such as stochastic programming [9], [10], chance constrained programming [11], [12], and robust optimization [13], [14] have been widely used to handle with the uncertainties in decision making. Robust optimization has gotten the popularity in recent research due to its computational efficiency [15]. In robust optimization, each point in the uncertainty set is a possible realization of the uncertainties, and the goal is to optimize the worst case, which is often too conservative [15]. To reduce the conservatism, lots of machine learning methods for adjusting the uncertainty set size were integrated into the robust optimization framework, such as kernel learning [16], principal component analysis [17], and Dirichlet process mixture model [18]. With the application of machine learning methods, many advanced data-driven optimization frameworks under uncertainty have also been proposed [19].

In robust optimization, all decisions are made before the uncertain data are known and

represented as “here and now” decisions. In real-world applications, some auxiliary variables can be determined when part of the uncertainty is revealed, viewed as “wait and see” decisions. These variables can adjust themselves to the corresponding uncertain data. Although this mechanism can reduce conservatism, the multilevel robust optimization problem is sometimes computationally intractable. To deal with this difficulty, affine functions were introduced to reformulate a computationally tractable two-stage robust counterpart, and a less conservative solution was obtained [20]. Based on that, lots of adaptive robust optimization (ARO) methods have been proposed [18]. The ARO method has been widely used in process and energy system optimization, including the security constrained unit commitment problem [21], multi-period economic dispatch of power systems [22], planning and scheduling under uncertainty [23], and scheduling of batch manufacturing processes [24]. Zhao et al. [25] presented a two-stage ARO approach for the operational optimization of a steam system with uncertain steam turbine model parameters. These studies show that applying two-stage ARO in real optimization problems can reduce the conservatism and achieve better solutions.

With the application of machine learning methods, data-driven robust optimization and ARO have been integrated into process and energy system optimization under uncertainty [26],[27]. However, due to the complex units mechanism and connections in the industrial energy systems, the industrial multi-type energy system optimization under uncertainty is still lack. On account of the specific structure and characteristics of the industrial energy system, the methods developed on power systems can not be directly transferred to them. In addition, the distribution of industrial data can not be treated as a normal one, which requires appropriate uncertain parameters derivation and uncertainty set construction methods based on multi-field specialized knowledge.

In the energy system of an industrial ethylene plant, the three most important steam turbines are designed to drive the cracked gas compressor, propylene refrigeration compressor, and ethylene refrigeration compressor, respectively. The power demands of these compressors are significantly affected by the operational conditions of the cracked gas compression system and chilling train system. However, the solution of deterministic optimization may be infeasible, especially when the real demands are higher than the nominal ones. In this study, typical operational conditions during more than two years were collected from the industrial process historical database (PHD), and the corresponding process mechanical power demands of the three main compressors were calculated by using Aspen Plus[®] [28]. Given that uncertain parameters cannot be predefined, a two-stage ARO framework for the operational optimization of the industrial multi-type energy system under demand uncertainty was proposed. The deterministic energy system optimization model was formulated based on the process mechanism and industrial characteristics. RKDE [29] was then applied to construct the uncertainty set. A data-driven two-stage adaptive robust MINLP model was

developed afterward for the operating optimization of the energy system under demand uncertainty. By using the affine decision rule (ADR), the robust counterpart of the ARO model was formulated as a computationally tractable single-level MINLP model. A case study of a practical energy system in ethylene manufacturing was also performed to demonstrate the efficiency of the proposed method.

The main novelties are as follows:

(1) A two-stage ARO framework combining robust optimization and machine learning methods was presented to address the uncertainty in the industrial multi-type energy system.

(2) Deterministic and data-driven ARO models were developed by combining the process mechanism and operation characteristics.

(3) The industrial data were obtained from an actual ethylene plant, and RKDE was used to construct the uncertainty set.

(4) A case study was performed on an actual multi-type energy system of an ethylene plant.

2. Problem statement

As shown in Fig.1, the multi-type energy system of an industrial ethylene plant comprises a steam generation system, a steam turbine network, an electric power system, and a cooling water system. There are four types of energy (fuel, steam, electricity, and water) transformed and transported in this system. The waste heat recovery system (WHRS) is a simplification of the cracking and SS generation system. Although most of the SS demand can be satisfied by the WHRS, there are some boilers (BO) for additional SS supply. Fuel and water are consumed in both the WHRS and boilers. Several types of turbines such as extraction-condensing turbines, back-pressure turbines, and fully condensing turbines constitute the steam turbine network. Low process mechanical power demands are met by either steam turbine (ST) or standby electric motors. ST1, ST2, and ST3 are designed to drive the cracked gas compressor, propylene refrigeration compressor, and ethylene refrigeration compressor, respectively. However, letdown valves (LV) are employed for the steam network balance, which is a waste of energy. The performance of the extraction-condensing turbines and fully condensing turbines can be greatly affected by the operational conditions of the cold end. Although reducing the cooling water temperature can improve the work produced by steam turbines, the electricity consumption in the cooling water system will increase. The cross-flow cooling towers (CT) with electric motors (MT) are used for cooling the returned water. Cooling water collected in the water sink are transported by electric pumps (PU) to the users.

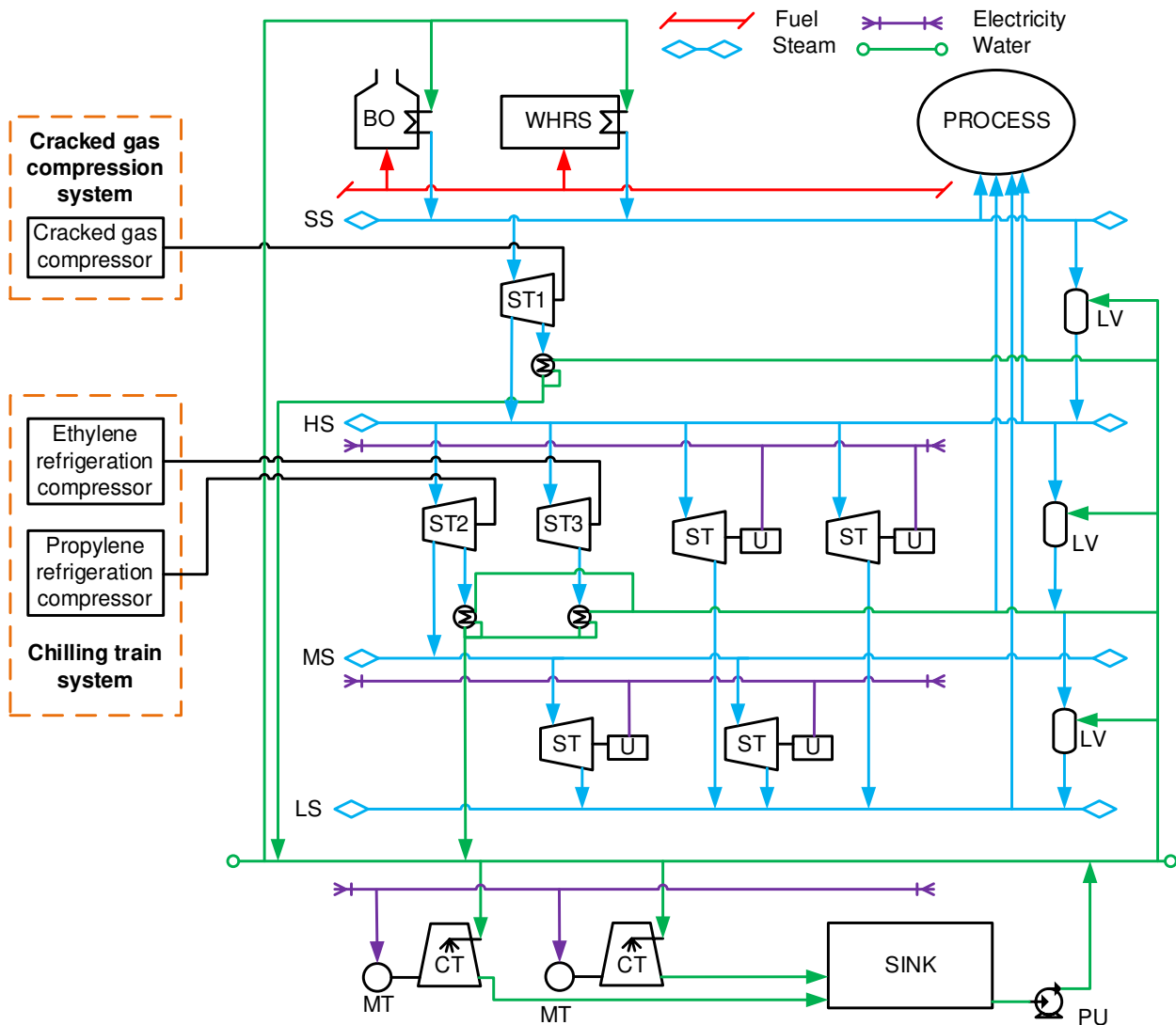


Fig. 1. Basic structure of the industrial multi-type energy system

The energy system optimization problem studied in this paper is stated as: given the following information (1) regressed parameters of unit efficiency functions; (2) mass flowrates of fuel, SS, and water in the WHRS; (3) multilevel steam demands; (4) rated powers of the cooling tower motors and water pump; (5) local meteorological conditions (environmental temperature and humidity); (6) energy weighting coefficients; and (7) process historical data of the cracked gas compression and chilling train systems, including key flowrates, temperatures, and pressures, the objective is minimizing the weighted total energy consumption under uncertain mechanical power demands. The decision variables were selected according to practical operability and sensitivity analysis, which include mass flowrate of the SS produced in steam boilers, mass flowrate of extraction steam of turbines, mass flowrate of inlet steam of the letdown valves, and binary variables indicating whether the units are applied. The decision variables were optimized to satisfy the process demands more efficiently, which will have little effect on the ethylene yield. The uncertain requirements in the power demand constraints were derived based on the PHD of an

actual ethylene plant.

3. Deterministic model of the energy system

An accurate model is essential for energy system optimization. By combining the process unit mechanism and industrial historical data, a novel deterministic energy system optimization model is formulated [3]. In this system, boilers efficiencies were regressed as Eq. (1) [4] by using industrial historical data.

$$\eta_{bo} = \frac{M_{bo,water}^{in} / M_{bo,water}^{max}}{(1 + \beta_{bo})(M_{bo,water}^{in} / M_{bo,water}^{max}) + \alpha_{bo}}, \quad \forall bo \in BO \quad (1)$$

where α_{bo} and β_{bo} are the parameters in the regress function, $M_{bo,water}^{in}$ and $M_{bo,water}^{max}$ represent the mass flowrate of inlet water and maximum load of boiler bo .

In general, the work produced by a multiple extraction steam turbine can be calculated as

$$G_{st}^{tur} = (M_{st}^{ext} + M_{st}^{out})H_{st}^{in} - M_{st}^{ext}H_{st}^{ext} - M_{st}^{out}H_{st}^{out}, \quad \forall st \in ST \quad (2)$$

where G_{st}^{tur} is the power produced by the steam turbine st , M_{st}^{ext} and M_{st}^{out} are the mass flowrate of the extraction and outlet steam, and H_{st}^{in} , H_{st}^{ext} , and H_{st}^{out} are the enthalpies of corresponding streams.

Steam condensers are key components of the cold-end system of the extraction-condensing turbines, and the performance of steam condensers is affected by the cooling water temperature. The steam condensers were modeled based on the revised logarithm mean temperature difference as defined in Eqs. (3) to (7).

$$Q_{stc} = KA_{stc} \Delta t_{m,stc} = M_{stc,water} cp_{water} \Delta t_{stc} \quad (3)$$

$$\Delta t_{m,stc} = \frac{(T_{steam}^{out} - T_{cw}) - (T_{steam}^{out} - T_{rw})}{\ln[(T_{steam}^{out} - T_{cw}) / (T_{steam}^{out} - T_{rw})]} = \frac{\Delta t_{stc}}{\ln((\Delta t_{stc} + \delta t_{stc}) / \delta t_{stc})} \quad (4)$$

$$T_{rw,stc} = T_{cw,stc} + \Delta t_{stc} + \delta t_{stc} \quad (5)$$

$$P_{stc}^{sat} = 0.00981 \left(\frac{T_{rw,stc} + 100}{57.66} \right)^{7.46} \quad (6)$$

$$H_{st}^{out} = f_{H_{st}^{out}}(P_{stc}^{sat}), \quad \forall st \in ST, \quad \forall stc \in STC \quad (7)$$

where Q_{stc} is the heat transferred in the steam condenser, KA_{stc} is the heat transfer coefficient and heat transfer area, $\Delta t_{m,stc}$ is the revised logarithm mean temperature difference, $M_{stc,water}$ is the mass flowrate of water, T_{steam}^{out} , T_{cw} , and T_{rw} are the temperatures of the outlet steam of turbine, inlet cooling water, and outlet returned water, respectively, Δt_{stc} is the water temperature difference, δt_{stc} is the terminal temperature difference of steam condensers, $f_{H_{st}^{out}}(P_{stc}^{sat})$ is a

regression function of H_{st}^{out} vs P_{stc}^{sat} , and P_{stc}^{sat} is the saturated vapor pressure under $T_{rw,stc}$ calculated by the empirical formula [30].

Although letdown valves are indispensable parts for steam network balance, reducing the opening can avoid unnecessary energy waste. By combining the mass and energy balance, the mass flowrate of the outlet steam of the LVs can be represented as

$$M_{lv,steam}^{out} = \left(H_{lv,steam}^{in} - H_{lv,water} \right) / \left(H_{lv,steam}^{out} - H_{lv,water} \right) \cdot M_{lv,steam}^{in}, \quad \forall lv \in LV \quad (8)$$

where $M_{lv,steam}^{in}$ and $M_{lv,steam}^{out}$ are the mass flowrate of inlet and outlet steam, $H_{lv,steam}^{in}$ and $H_{lv,steam}^{out}$ are the enthalpies of inlet and outlet steam and $H_{lv,water}$ is the enthalpy of water in the letdown valves.

The cooling water system comprises cross-flow cooling towers equipped with rated power motors, water pumps, and a water collecting sink. The heat balance of the cooling tower was formulated as Eqs. (9) to (11).

$$Q_{ct,air} = \left(M_{ct,air} + M_{ct,vapor} \right) cp_{ct,air}^{out} T_{ct,air}^{out} - M_{ct,air} cp_{ct,air}^{in} T_{ct,air}^{in}, \quad \forall ct \in CT \quad (9)$$

$$Q_{ct,vapor} = M_{ct,vapor} r_{water}, \quad \forall ct \in CT \quad (10)$$

$$Q_{water} = \eta_{ct} \sum_{ct} z_{ct} \left(Q_{ct,air} + Q_{ct,vapor} \right) \quad (11)$$

where $Q_{ct,air}$ and $Q_{ct,vapor}$ are the heat exchanged with air and taken by water evaporation, $M_{ct,air}$ and $M_{ct,vapor}$ are the mass flowrate of air and vapor, $cp_{ct,air}^{in}$ and $cp_{ct,air}^{out}$ are the specific heat capacity of the inlet and out air, $T_{ct,air}^{in}$ and $T_{ct,air}^{out}$ are the temperature of the inlet and out air, r_{water} is the latent heat of water, Q_{water} is the heat taken from the inlet water and η_{ct} is the cooling tower efficiency.

The cooling tower efficiency regression function was proposed in our previous work [3] as Eq. (12), which considered the effect of cooling water temperature, inlet air temperature and cooling tower load

$$\eta_{ct} = \left(\varepsilon_{ct} \left(T_{cw} - T_{ct,air}^{in} \right) + \phi_{ct} \right) \cdot \frac{\varphi_{ct} M_{ct,water}^{in} / M_{ct,water}^{\max}}{1 - \gamma_{ct} M_{ct,water}^{in} / M_{ct,water}^{\max}}, \quad \forall ct \in CT \quad (12)$$

where ε_{ct} , ϕ_{ct} , φ_{ct} , and γ_{ct} are the parameters. The cooling water temperature can be calculated by using Eq. (13). Fresh water is used to make up for the vapor loss in the cooling towers and the blowdown of sink M_{blw} . The mass flowrate of required fresh water M_{cfw} was calculated using Eq. (14).

$$T_{cw} = T_{rw} - \frac{Q_{water}}{cp_{water}} \quad (13)$$

$$M_{cfw} = \sum_{ct} z_{ct} M_{ct,vapor} + M_{bbw} \quad (14)$$

The process mechanical power demands constraint is shown in Eq. (15), where the demands were met by the matching steam turbines or the standby electric motors.

$$z_{st} \left((H_{st}^{in} - H_{st}^{ext}) M_{st}^{ext} + (H_{st}^{in} - H_{st}^{out}) M_{st}^{out} \right) + (1 - z_{st}) G_{st}^{mt} \geq G_{st}^{user} \quad (15)$$

where G_{st}^{user} is the power demand, and G_{st}^{mt} is the power provided by the standby electric motors.

The multilevel steam balance in the steam pipe network is expressed in Eqs. (16) to (19).

$$\sum_{bo} z_{bo} M_{bo,wat}^{in} + M_{whrs,ss}^{out} \geq \sum_{st} z_{st} M_{st,ss}^{in} + \sum_{lv} M_{lv,ss}^{in} \quad (16)$$

$$\sum_{st} z_{st} M_{st,ss}^{ext} + \sum_{lv} M_{lv,ss}^{out} + M_{hs,im} \geq \sum_{st} z_{st} M_{st,hs}^{in} + \sum_{lv} M_{lv,hs}^{in} + M_{hs}^{pro} \quad (17)$$

$$\sum_{st} z_{st} M_{st,hs}^{ext} + \sum_{lv} M_{lv,hs}^{out} + M_{ms,im} \geq \sum_{st} z_{st} M_{st,ms}^{in} + \sum_{lv} M_{lv,ms}^{in} + M_{ms}^{pro} \quad (18)$$

$$\sum_{st} z_{st} M_{st,ms}^{ex} + \sum_{lv} M_{lv,ms}^{out} \geq M_{ls}^{pro} \quad (19)$$

where M_{hs}^{pro} , M_{ms}^{pro} , and M_{ls}^{pro} are the process steam demands, $M_{hs,im}$ and $M_{ms,im}$ are the mass flowrate of imported HS and MS.

The decision variables ranges were set according to the normal operational conditions:

$$y^{\min} \leq y \leq y^{\max} \quad (20)$$

The fuel is mainly consumed in the boilers and WHRS. Steam consumption includes HS and MS consumption, which can be imported from or sold to other plants. Electricity is consumed in the mechanical power user standby motors and cooling tower equipped motors. Water is used in the steam boilers and the WHRS for producing SS, in the water network as a supplement, and in letdown valves for downgrading steam. z_{bo} , z_{st} , z_{mt} , and z_{pu} are binary variables that indicate whether the candidate boilers, steam turbines, cooling tower motors, pumps are applied, respectively. The objective is to minimize the weighted total energy consumption.

$$\min C_{total} = \zeta_{fuel} C_{fuel} + \zeta_{HS} C_{HS} + \zeta_{MS} C_{MS} + \zeta_{electricity} C_{electricity} + \zeta_{water} C_{water} \quad (21)$$

where ζ_{fuel} , ζ_{HS} , ζ_{MS} , $\zeta_{electricity}$, and ζ_{water} are the corresponding weighting coefficients.

The accuracy of the energy system model has been proved in [3]. Based on the device models and system constraints, the deterministic energy system optimization model was formulated as an MINLP problem:

$$\begin{aligned}
& \min C_{total} \\
& \text{s.t. Mass and energy constraints in Eqs. (1)-(14)} \\
& \quad \text{Power requirement constraint in Eq. (15)} \\
& \quad \text{Steam network balance constraints in Eqs. (16)-(19)} \\
& \quad \text{Variables range constraint in Eq. (20)}
\end{aligned} \tag{22}$$

4. Data-driven two-stage ARO model of the energy system

In industrial plants, the process mechanical power demands are uncertain and significantly affected by the operational conditions of the process. The uncertain parameters in the energy system are the deviation (ε_1 , ε_2 and ε_3) of the real process mechanical power demands from their nominal values, which can be represented as the vector $\varepsilon = [\varepsilon_1 \ \varepsilon_2 \ \varepsilon_3]^T$. The procedure for deriving uncertain parameters is illustrated in Fig.2. The key operational parameters of the cracked gas compression system and chilling train system over more than two years were collected from process historical database, which covers most typical operational conditions. The data with gross error was removed, and the rest data was reconciled before use. The processed data were imported into the cracked gas compression system and chilling train system models. By running the Aspen Plus® models, the process mechanical power demands were derived, and the uncertain deviation was calculated.

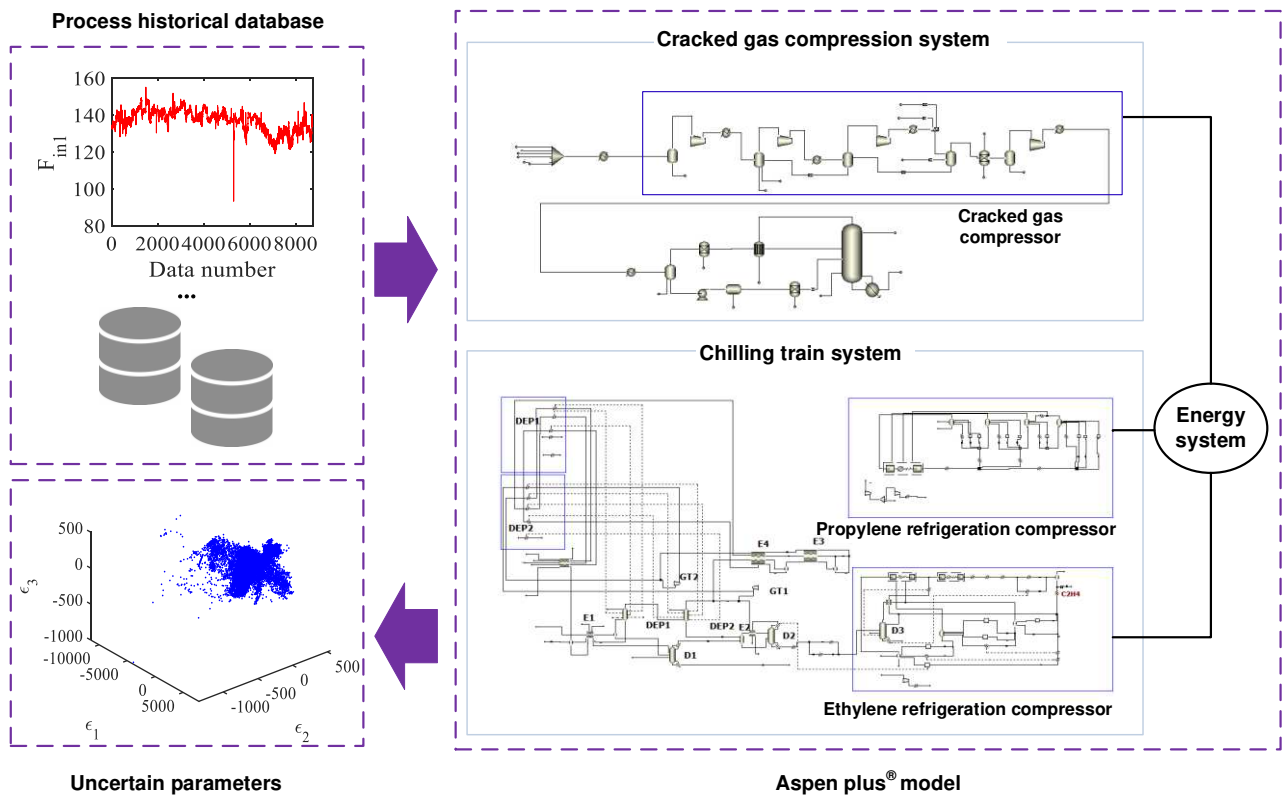


Fig. 2. Procedure of deriving uncertain parameters of the energy system

As demonstrated in Fig.2, the uncertain parameters are correlated and non-evenly distributed.

Therefore, a linear or nonlinear function can hardly capture the characteristics of the data. RKDE [31] was applied to construct the uncertainty set using the derived uncertain parameters, which can efficiently extract distributional information of the uncertain parameters. RKDE can enhance the performance of KDE by introducing a robust loss function [32] and has been widely used in process and energy system optimization problems.

The KDE of the density function f of uncertain parameters can be represent as Eq. (23), where $\mathbf{v}_{(1)}, \dots, \mathbf{v}_{(N)} \in R^d$ is N realizations of the uncertainties [33].

$$\hat{f}_{KDE}(\mathbf{v}) = \frac{1}{N} \sum_{i=1}^N K_b(\mathbf{v}, \mathbf{v}_{(i)}) \quad (23)$$

K_b is a kernel function with bandwidth b . Here a popular Gaussian kernel function [32] was adopted

$$K_b(\mathbf{v}, \mathbf{v}_{(i)}) = \left(\frac{1}{\sqrt{2\pi}b} \right)^d \exp\left(-\frac{\|\mathbf{v} - \mathbf{v}_{(i)}\|^2}{2b^2} \right) \quad (24)$$

There is a mapping Φ from R^d to H such that $K_b(\mathbf{v}, \mathbf{v}_{(i)}) = \langle \Phi(\mathbf{v}), \Phi(\mathbf{v}_{(i)}) \rangle$ as the Gaussian kernel is a positive semi-definite kernel [32]. H is an infinite dimensional Hilbert space of functions. Therefore, the KDE can be obtained by solving the least squares problem

$$\min_{h \in H} \sum_{i=1}^N \|\Phi(\mathbf{v}_{(i)}) - h\|^2 \quad (25)$$

where h is a function in H . Noting that the loss function in the KDE is quadratic, which is sensitive to the outliers. To deal with this issue, the RKDE method was employed and it can be regarded as the solution of the minimization problem Eq. (26) using a kernelized iteratively reweighted least squares algorithm [32].

$$\min_{h \in H} J(h) = \sum_{i=1}^N \delta\left(\|\Phi(\mathbf{v}_{(i)}) - h\|\right) \quad (26)$$

where $\delta(\cdot)$ is the robust loss function. A widely used Hampel loss function [34] was then adopted. For i th component in the uncertainty set ε_i , $\hat{F}_{RKDE}^i(\varepsilon_i)$ is the cumulative density function, while the quantile function was derived by using Eq. (27). The quantile function returned a minimum ε_i according to the predefined parameter α , and the confidence level was $(1-2\alpha)$.

$$\hat{F}_{RKDE}^{i-1}(\alpha) = \min\{\varepsilon_i \in R \mid \hat{F}_{RKDE}^i(\varepsilon_i) \geq \alpha\} \quad (27)$$

The data-driven uncertainty set constructed using the quantile function was formulated as Eq. (28), where θ is the uncertainty budget to control the level of conservatism, and ε_i^0 and φ_i are

the center of the uncertainty set and the relative deviation, respectively, which can be calculated by using Eqs. (29) and (30).

$$U = \left\{ \boldsymbol{\varepsilon} \left| \begin{array}{l} \hat{F}_{RKDE}^{i-1}(\alpha) \leq \varepsilon_i \leq \hat{F}_{RKDE}^{i-1}(1-\alpha), \quad \forall i \\ \sum_i \varepsilon_i^0 (1-\varphi_i \theta) \leq \sum_i \varepsilon_i \leq \sum_i \varepsilon_i^0 (1+\varphi_i \theta) \end{array} \right. \right\} \quad (28)$$

$$\varepsilon_i^0 = \left(\hat{F}_{RKDE}^{i-1}(\alpha) + \hat{F}_{RKDE}^{i-1}(1-\alpha) \right) / 2 \quad (29)$$

$$\varphi_i = \left(\hat{F}_{RKDE}^{i-1}(1-\alpha) - \varepsilon_i^0 \right) / \varepsilon_i^0 \quad (30)$$

The box-based and RKDE-based uncertainty sets are presented in Fig.3. The RKDE-based method can provide a compact set, while the box-based uncertainty set covers plenty of unnecessary space. The RKDE-based approach can capture the region with real high values of the probability density function, thereby significantly reducing conservatism.

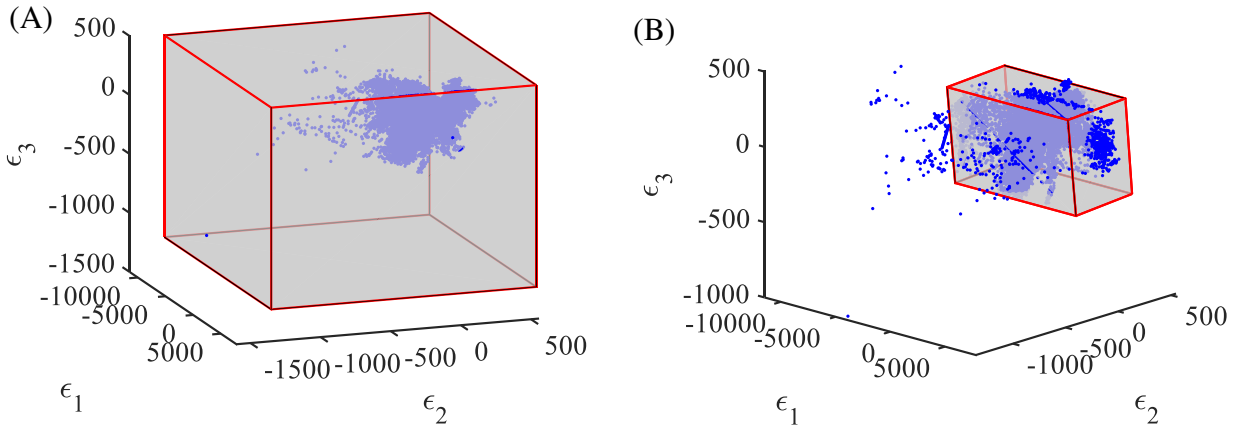


Fig. 3. The constructed uncertainty set: (A) box-based uncertainty set; and (B) RKDE-based uncertainty set

A data-driven adaptive robust energy system optimization model was then developed based on the derived uncertainty set. Generally, a two-stage robust optimization problem can be formulated as Eq. (31), where \mathbf{x} is the first-stage decision variables, which may contain integer and continuous variables. In the two-stage robust optimization framework, the second-stage decision variables were determined after part of the uncertainty is revealed.

$$\begin{aligned} \min_{\mathbf{x}} \quad & \mathbf{c}^T \mathbf{x} + \max_{\boldsymbol{\varepsilon} \in U} l(\mathbf{x}, \boldsymbol{\varepsilon}) \\ \text{s.t.} \quad & \mathbf{A} \mathbf{x} \leq \mathbf{b} \end{aligned} \quad (31)$$

Considering a linear programming second-stage sub-problem (Eq. (32)), where \mathbf{y} denotes the continuous variables to be determined after the uncertainty $\boldsymbol{\varepsilon}$ is revealed. The ADR [20] was applied to derive a robust counterpart of the two-stage ARO problem.

$$l(\mathbf{x}, \boldsymbol{\varepsilon}) = \begin{cases} \min_{\mathbf{y}} \quad \mathbf{d}^T \mathbf{y} \\ \text{s.t.} \quad \mathbf{T}(\boldsymbol{\varepsilon}) \mathbf{x} + \mathbf{W} \mathbf{y} \leq \mathbf{h}(\boldsymbol{\varepsilon}) \end{cases} \quad (32)$$

In the constraint of Eq. (32), \mathbf{T} , \mathbf{h} , and \mathbf{y} are affinely influenced by uncertainties. By applying

ADR, these parameters can be represented by Eqs. (33) to (35), respectively. The matrix form of Eq. (35) can be arranged as Eq. (36).

$$\mathbf{T}_j(\boldsymbol{\varepsilon}) = \mathbf{T}_j^0 + \sum_i \varepsilon_i \mathbf{T}_{ji}^\varepsilon \quad (33)$$

$$\mathbf{h}(\boldsymbol{\varepsilon}) = \mathbf{h}^0 + \sum_i \varepsilon_i \mathbf{h}_i^\varepsilon \quad (34)$$

$$y_k(\boldsymbol{\varepsilon}) = y_k^0 + \sum_i \varepsilon_i y_{ki}^\varepsilon \quad (35)$$

$$\mathbf{y}(\boldsymbol{\varepsilon}) = \mathbf{y}^0 + \mathbf{Y}^\varepsilon \boldsymbol{\varepsilon} \quad (36)$$

By integrating Eqs. (33) to (36), a conservative approximation to the two-stage ARO problem in Eq. (32) can be derived as Eq. (37).

$$\begin{aligned} \min_{\mathbf{x}} \quad & \max_{\mathbf{y}, \boldsymbol{\varepsilon} \in U} \mathbf{c}^T \mathbf{x} + \mathbf{d}^T \mathbf{y}(\boldsymbol{\varepsilon}) \\ \text{s.t.} \quad & \mathbf{A} \mathbf{x} \leq \mathbf{b} \\ & \mathbf{T}(\boldsymbol{\varepsilon}) \mathbf{x} + \mathbf{W} \mathbf{y}(\boldsymbol{\varepsilon}) \leq \mathbf{h}(\boldsymbol{\varepsilon}) \end{aligned} \quad (37)$$

An epigraph reformulation of Eq. (37) was developed as Eq. (38), to deal with the uncertain parameters in the objective function.

$$\begin{aligned} \min_{\mathbf{x}, \mathbf{y}} \quad & q \\ \text{s.t.} \quad & \mathbf{c}^T \mathbf{x} + \mathbf{d}^T \mathbf{y}(\boldsymbol{\varepsilon}) \leq q, \quad \forall \boldsymbol{\varepsilon} \in U \\ & \mathbf{T}(\boldsymbol{\varepsilon}) \mathbf{x} + \mathbf{W} \mathbf{y}(\boldsymbol{\varepsilon}) \leq \mathbf{h}(\boldsymbol{\varepsilon}), \quad \forall \boldsymbol{\varepsilon} \in U \\ & \mathbf{A} \mathbf{x} \leq \mathbf{b} \end{aligned} \quad (38)$$

To solve the resulting two-stage MINLP problem, the robust counterpart was derived. By defining $\hat{F}_{RKDE}^{i-1}(\alpha) = \varepsilon_i^{\min}$, $\hat{F}_{RKDE}^{i-1}(1-\alpha) = \varepsilon_i^{\max}$, $\sum_i \varepsilon_i^0 (1 - \varphi_i \theta) = \varepsilon^{\min, sum}$, and $\sum_i \varepsilon_i^0 (1 + \varphi_i \theta) = \varepsilon^{\max, sum}$, the uncertainty set U can be converted into Eqs. (39) to (42).

$$\varepsilon_i \leq \varepsilon_i^{\max} \quad (39)$$

$$-\varepsilon_i \leq -\varepsilon_i^{\min} \quad (40)$$

$$\sum_i \varepsilon_i \leq \varepsilon^{\max, sum} \quad (41)$$

$$-\sum_i \varepsilon_i \leq -\varepsilon^{\min, sum} \quad (42)$$

By applying ADR $\mathbf{y}(\boldsymbol{\varepsilon}) = \mathbf{y}^0 + \mathbf{Y}^\varepsilon \boldsymbol{\varepsilon}$, the first constraint in Eq. (38) was reformulated as

$$\max_{\boldsymbol{\varepsilon} \in U} \mathbf{d}^T \mathbf{Y}^\varepsilon \boldsymbol{\varepsilon} \leq q - \mathbf{c}^T \mathbf{x} - \mathbf{d}^T \mathbf{y}^0 \quad (43)$$

Given that the left-hand side of Eq. (43) is a linear programming, by introducing dual variables γ_i , η_i , κ , and λ , Eq. (43) was reformulated as Eqs. (44) to (46).

$$\sum_i \varepsilon_i^{\max} \gamma_i - \sum_i \varepsilon_i^{\min} \eta_i + \varepsilon^{\text{sum,max}} \kappa - \varepsilon^{\text{sum,min}} \lambda \leq q - \mathbf{c}^T \mathbf{x} - \mathbf{d}^T \mathbf{y}^0 \quad (44)$$

$$\gamma_i - \eta_i + \kappa - \lambda = \mathbf{d}^T \mathbf{Y}^\varepsilon, \quad \forall i \quad (45)$$

$$\gamma_i, \eta_i, \kappa, \lambda \geq 0, \quad \forall i \quad (46)$$

Similarly, the second constraint in Eq. (38) was reformulated as Eq. (47) based on ADR.

$$(\mathbf{T}^\varepsilon \mathbf{x} + \mathbf{WY}^\varepsilon - \mathbf{h}^\varepsilon) \boldsymbol{\varepsilon} \leq \mathbf{h}^0 - \mathbf{T}^0 \mathbf{x} - \mathbf{W}\mathbf{y}^0 \quad (47)$$

The left-hand side of Eq. (47) is a linear programming. By introducing dual variables τ_i , ν_i , ω , and ψ , Eq. (47) was reformulated as

$$\sum_i \varepsilon_i^{\max} \tau_i - \sum_i \varepsilon_i^{\min} \nu_i + \varepsilon^{\text{sum,max}} \omega - \varepsilon^{\text{sum,min}} \psi \leq \mathbf{h}^0 - \mathbf{T}^0 \mathbf{x} - \mathbf{W}\mathbf{y}^0 \quad (48)$$

$$\tau_i - \nu_i + \omega - \psi = \mathbf{T}^\varepsilon \mathbf{x} + \mathbf{WY}^\varepsilon - \mathbf{h}^\varepsilon, \quad \forall i \quad (49)$$

$$\tau_i, \nu_i, \omega, \psi \geq 0, \quad \forall i \quad (50)$$

The objective to minimize total energy consumption in Eq. (21) can be reformulated as Eq. (51), where the second-stage cost $C_{total,2} = \mathbf{P}\mathbf{y}(\boldsymbol{\varepsilon})$ is determined after part of the uncertainty is revealed.

$$\begin{aligned} & \min_{\mathbf{x}} C_{total,1}(\mathbf{x}) + \max_{\mathbf{y}, \boldsymbol{\varepsilon} \in U} C_{total,2}(\mathbf{y}, \boldsymbol{\varepsilon}) \\ & s.t. \quad \mathbf{A}\mathbf{x} \leq \mathbf{b} \\ & \quad \mathbf{T}(\boldsymbol{\varepsilon})\mathbf{x} + \mathbf{W}\mathbf{y} \leq \mathbf{h}(\boldsymbol{\varepsilon}) \end{aligned} \quad (51)$$

According to the epigraph reformulation in Eq. (38), the two-stage adaptive robust energy system optimization model in Eq. (51) was rewritten as Eq. (52). The constraint in Eq. (52) can be reformulated as Eq. (53) based on ADR.

$$\begin{aligned} & \min_{\mathbf{x}, \mathbf{y}} q \\ & s.t. \quad C_{total,1}(\mathbf{x}) + \mathbf{P}\mathbf{y}(\boldsymbol{\varepsilon}) \leq q, \quad \forall \boldsymbol{\varepsilon} \in U \end{aligned} \quad (52)$$

$$\max_{\boldsymbol{\varepsilon} \in U} \mathbf{P}\mathbf{Y}^\varepsilon \boldsymbol{\varepsilon} \leq q - C_{total,1}(\mathbf{x}) - \mathbf{P}\mathbf{y}^0 \quad (53)$$

By introducing dual variables γ_i^{obj} , η_i^{obj} , κ^{obj} , and λ^{obj} , Eq. (53) was reformulated as

$$\sum_i \varepsilon_i^{\max} \gamma_i^{obj} - \sum_i \varepsilon_i^{\min} \eta_i^{obj} + \varepsilon^{\text{sum,max}} \kappa^{obj} - \varepsilon^{\text{sum,min}} \lambda^{obj} \leq q - C_{total,1}(\mathbf{x}) - \mathbf{P}\mathbf{y}^0 \quad (54)$$

$$\gamma_i^{obj} - \eta_i^{obj} + \kappa^{obj} - \lambda^{obj} = \mathbf{P}\mathbf{Y}^\varepsilon, \quad \forall i \quad (55)$$

$$\gamma_i^{obj}, \eta_i^{obj}, \kappa^{obj}, \lambda^{obj} \geq 0, \quad \forall i \quad (56)$$

The demand constraint Eq. (15) involving uncertain parameters can be compactly represented as

followers where $G_{st}^{user}(\boldsymbol{\varepsilon}) = \mathbf{y}^0 + \mathbf{Y}^\varepsilon \boldsymbol{\varepsilon}$, $\mathbf{H} = \begin{bmatrix} (H_{SS} - H_{HS})M_{st1}^{ext} + (H_{SS} - H_{sc1})M_{st1}^{out} \\ (H_{HS} - H_{MS})M_{st2}^{ext} + (H_{HS} - H_{sc2})M_{st2}^{out} \\ (H_{HS} - H_{sc3})M_{st3}^{out} \end{bmatrix}$.

$$\mathbf{y}^0 + \mathbf{Y}^\varepsilon \boldsymbol{\varepsilon} \leq \mathbf{H} \quad (57)$$

By introducing dual variables $\tau_{i,t}^{dem}$, $\nu_{i,t}^{dem}$, ω_t^{dem} , and ψ_t^{dem} , Eq. (57) was reformulated as constraints Eqs. (58) to (60), where t is the index of the power demand constraints.

$$\sum_i \varepsilon_i^{\max} \tau_{i,t}^{dem} - \sum_i \varepsilon_i^{\min} \nu_{i,t}^{dem} + \varepsilon^{sum,\max} \omega_t^{dem} - \varepsilon^{sum,\min} \psi_t^{dem} \leq H_t - \mathbf{y}_t^0, \quad \forall t \quad (58)$$

$$\tau_{i,t}^{dem} - \nu_{i,t}^{dem} + \omega_t^{dem} - \psi_t^{dem} = \mathbf{Y}_t^\varepsilon, \quad \forall i, t \quad (59)$$

$$\tau_{i,t}^{dem}, \nu_{i,t}^{dem}, \omega_t^{dem}, \psi_t^{dem} \geq 0, \quad \forall i, t \quad (60)$$

Based on the derived uncertain power demand constraint, the data-driven adaptive robust energy system optimization model can also be formulated as an MINLP problem:

$$\begin{aligned} & \min \max_{\varepsilon \in U} q \\ & \text{s.t.} \quad \text{Epigraph reformulation of objective function Eqs. (54)-(56)} \\ & \quad \text{Mass and energy constraints in Eqs. (1)-(14)} \\ & \quad \text{Power requirement constraint in Eqs. (58)-(60)} \\ & \quad \text{Steam network balance constraint in Eqs. (16)-(19)} \\ & \quad \text{Variables range constraint in Eq. (20)} \end{aligned} \quad (61)$$

5. Case study

5.1. Case description

A case study on a multi-type energy system of ethylene manufacturing was executed to prove the effectiveness of the proposed approach. The original structure and operational conditions of the studied energy system are presented in Fig. 4. One boiler, two HS-LS back-pressure turbines, two MS-LS back-pressure turbines, four water pumps, and six cooling towers were applied. The back-pressure turbines corresponding power users can also be driven by standby electric motors. The three most important steam turbines were designed to drive the cracked gas compressor, propylene refrigeration compressor, and ethylene refrigeration compressor, whose demands were calculated by the cracked gas compression system and chilling train system models. Other key process parameters are presented in Table 1, and the weighted coefficients of different types of energy were 1.05 kg oil/kg fuel, 0.08 kg oil/kg HS, 0.066 kg oil/kg MS, 2.3×10^{-4} kg oil/kW electricity, and 0.17 kg oil/ton water according to the industrial experience.

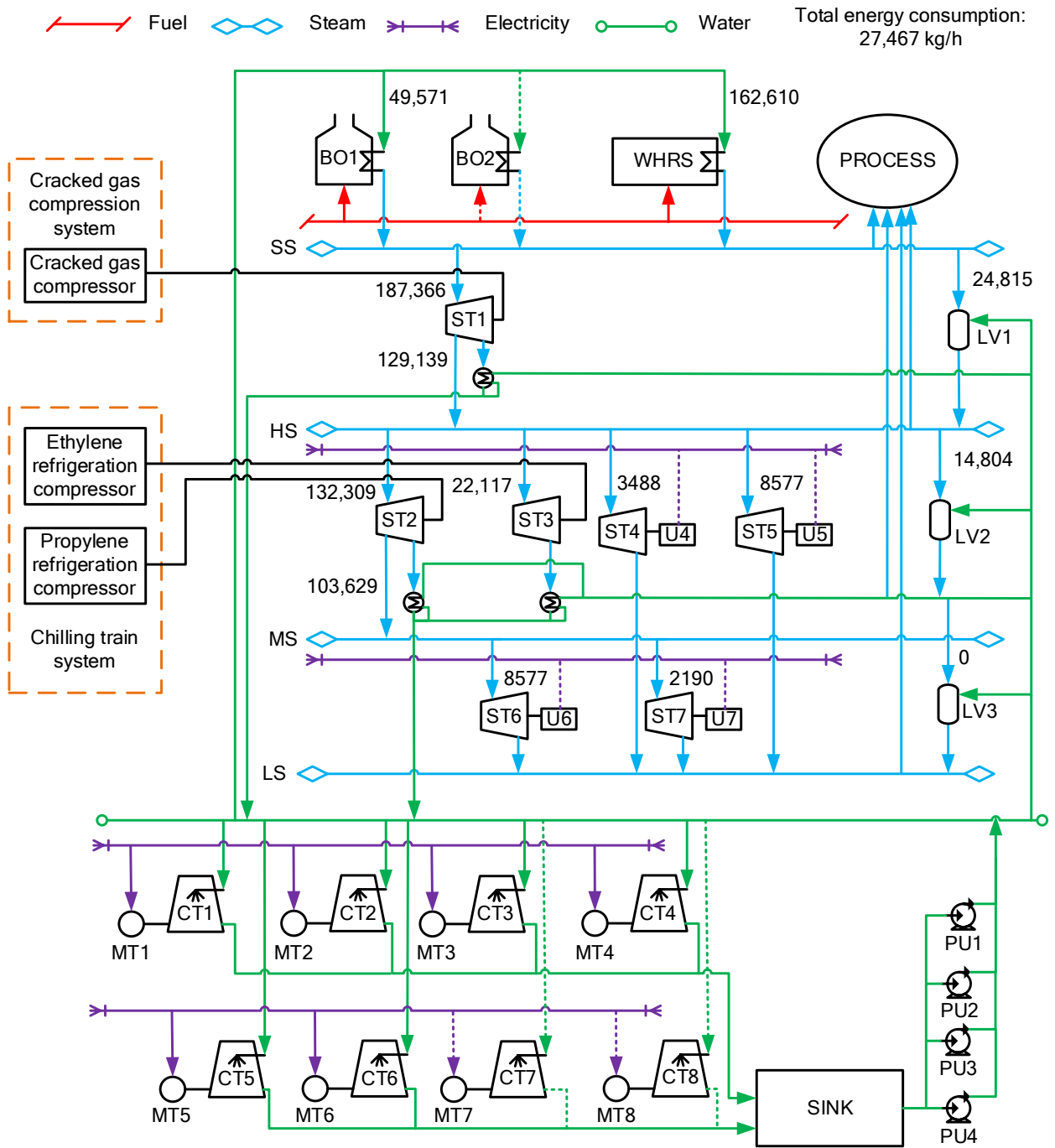


Fig. 4. Original structure and operational conditions of the energy system

Table 1. Process parameters in the energy system model

Parameters	Value	Parameters	Value
a_{bo} for $bo1$ - $bo2$	0.0851	Power demand of G_{st4}^{user} (kW)	297.45
b_{bo} for $bo1$ - $bo2$	0.0079	Power demand of G_{st5}^{user} (kW)	731.43
ε_{ct} for $ct1$ - $ct8$ in spring-autumn	0.03289	Power demand of G_{st6}^{user} (kW)	347.85
ϕ_{ct} for $ct1$ - $ct8$ in spring-autumn	0.475	Power demand of G_{st7}^{user} (kW)	88.83
φ_{ct} for $ct1$ - $ct8$ in spring-autumn	0.6915	Process demand of HS (kg/h)	21,727
γ_{ct} for $ct1$ - $ct8$ in spring-autumn	0.5807	Process demand of MS (kg/h)	55,176
Cooling towers motors efficiency η_{mt}	0.8	Process demand of LS (kg/h)	1466

There are 20,956 sets of historical process data collected from the ethylene plant to calculate the uncertain parameters based on the process models. Key input variables of the cracked gas compression system model are presented in Fig.5, where F^{in} is the inlet mass flowrate of the system, P^{in} , P_{stage1}^{out} , P_{stage2}^{out} , P_{stage3}^{out} , and P_{stage5}^{out} are the inlet pressure of the system, outlet pressure of stage1, stage2, stage3, and stage5, respectively. Key input variables of the chilling train system model are presented in Fig.6, where F_1^{in} is the mass flowrate of cracked gas from upstream, F_2^{in} is the mass flowrate of liquid from high pressure depropanizer condenser, and F_3^{in} is the mass flowrate of recycled ethane from ethylene splitter and F^S is the mass flowrate separated to Tail gas expander B; T_{C1}^{ovhd} , T_{C1}^{btm} , and T_{C1}^{sen} are the temperatures of the overhead stream, bottom stream, and sensitive stage of demethanizer prefractionator, respectively; T_{C2}^{ovhd} , and T_{C2}^{btm} are the temperatures of the overhead stream and bottom stream of Demethanizer, respectively.

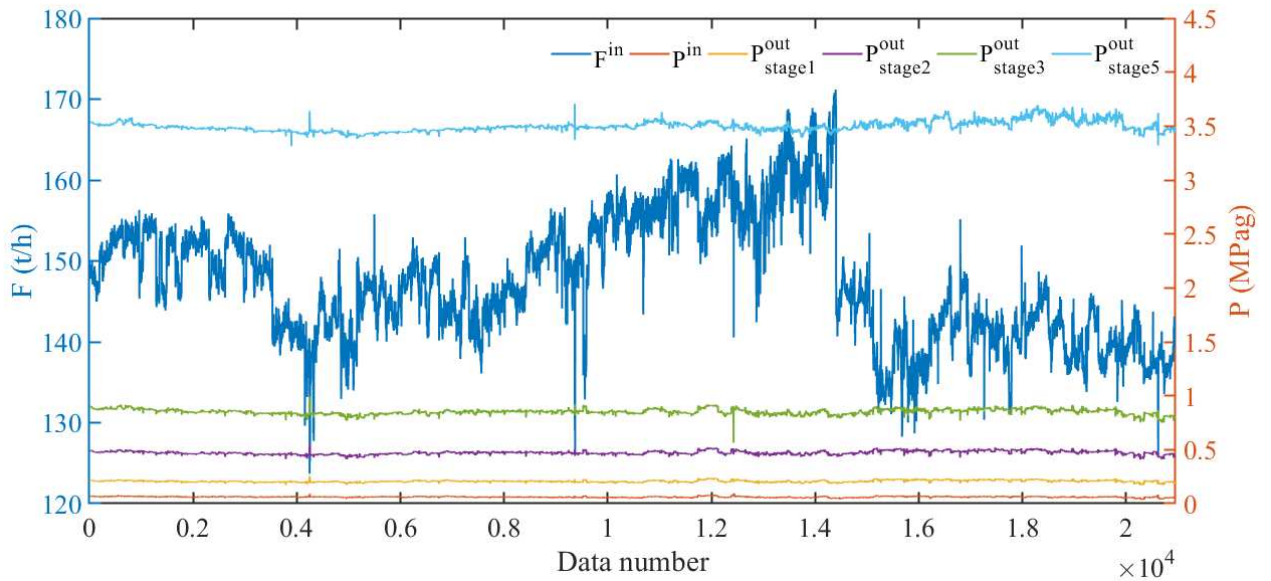


Fig. 5. Historical process data of the cracked gas compression system

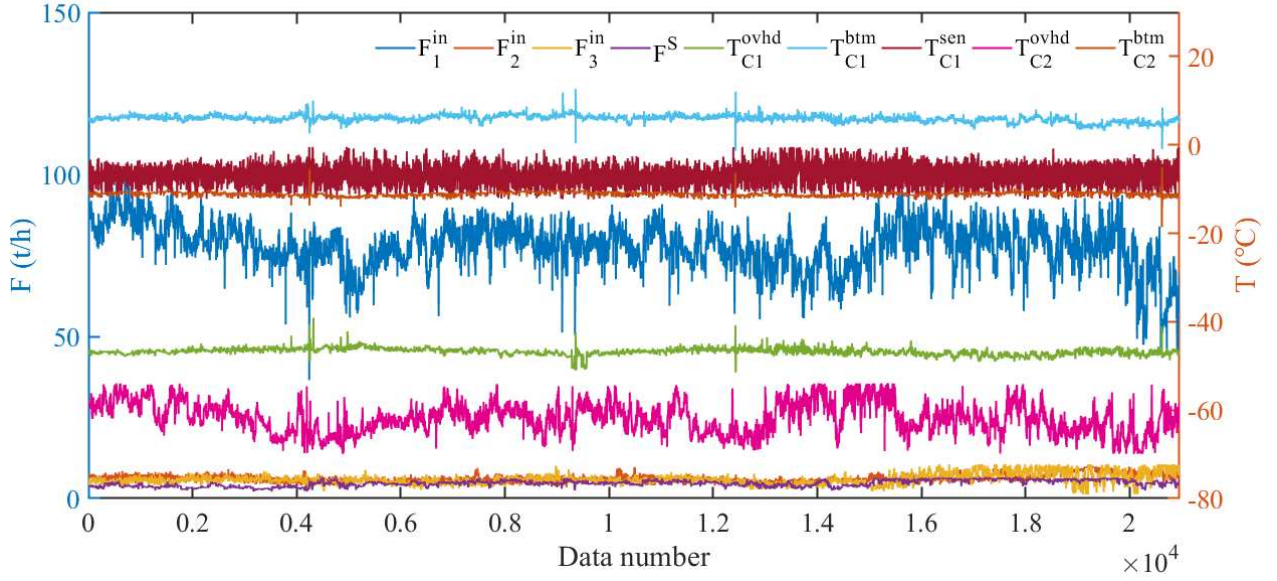


Fig. 6. Historical process data of the chilling train system

RKDE was used to construct the uncertainty set, where parameters α and θ were set as 0.1 and 0.2, respectively [25]. Given that $(1-2\alpha)$ is the confidence level, a larger α corresponds to a lower confidence level. Therefore, improving the value of α can generate a less conservative solution. The uncertainty budget θ denotes the degree of uncertainty deviation, and a larger θ increases the conservatism. A sensitivity analysis was performed to study the effect of the two parameters on the ARO solution. The nominal values of the process mechanical power demands were 19,094.85 kW, 8,133.85 kW, 3,606.27 kW. The boundary of the uncertain parameters is presented in Table 2.

Table 2. Boundary of uncertain parameters

	ε_1	ε_2	ε_3
Minimum value	-11480.86	-1351.85	-973.48
Maximum value	7821.54	537.87	357.16

5.2. Results and discussion

The deterministic and data-driven adaptive robust energy system optimization models (Eq. (22) and Eq. (61)) were coded in GAMS 24.7.4 and solved using the sub-solver Baron (16.8.24) [35] with the optimality tolerance of 0.01 %, which was implemented on a desktop with the Intel Core i9-10900k CPU @ 3.70 GHz and 64 GB memory. In the deterministic energy system optimization, the process mechanical power demands were set as their nominal values. In the Two-stage ARO with a box-based uncertainty set case, only the uncertainty parameters' boundary was considered. The problem sizes and solutions of different optimization methods are presented in Table 3. The ARO models had 43 additional continuous variables and 109 more constraints because of the introduction of auxiliary variables and application of ADR.

The price of robustness (PoR) [36] defined as $PoR = (obj_{nom} - obj_{ro}) / obj_{nom}$ was adopted as the measurement of the optimality level needs to be sacrificed for robustness, where obj_{nom} is the objective value of the deterministic optimization using nominal values and obj_{ro} is the objective value of the robust optimization. According to the definition, a lower value of PoR means less sacrifice of optimality for robustness, which is preferable. The deterministic optimal energy consumption was 25,509 kg/h given that only the nominal demands were considered. By applying RKDE, the proposed data-driven adaptive robust energy system optimization method obtained a solution of 26,064 kg/h and the PoR was only 2.18%, which is much less conservative than that using a box-based uncertainty set (PoR = 22.52%).

Table 3. Problem sizes and solutions of different optimization methods

	Deterministic optimization	Two-stage ARO with a box-based uncertainty set	Data-driven ARO with RKDE
Binary variables	18	18	18
Continuous variables	119	162	162
Constraints	110	219	219
Optimal energy consumption (kg/h)	25,509	31,253	26,064

The comparison of energy consumption under different optimization methods is shown in Fig. 7. Electricity and water always account for a small portion of total energy consumption. Fuel is the most important energy consumption, and more steam is imported under uncertain demands. Because of a compact uncertainty set in the proposed data-driven adaptive robust energy system optimization model, it results in less steam consumption of the system than the classical box-set based method.

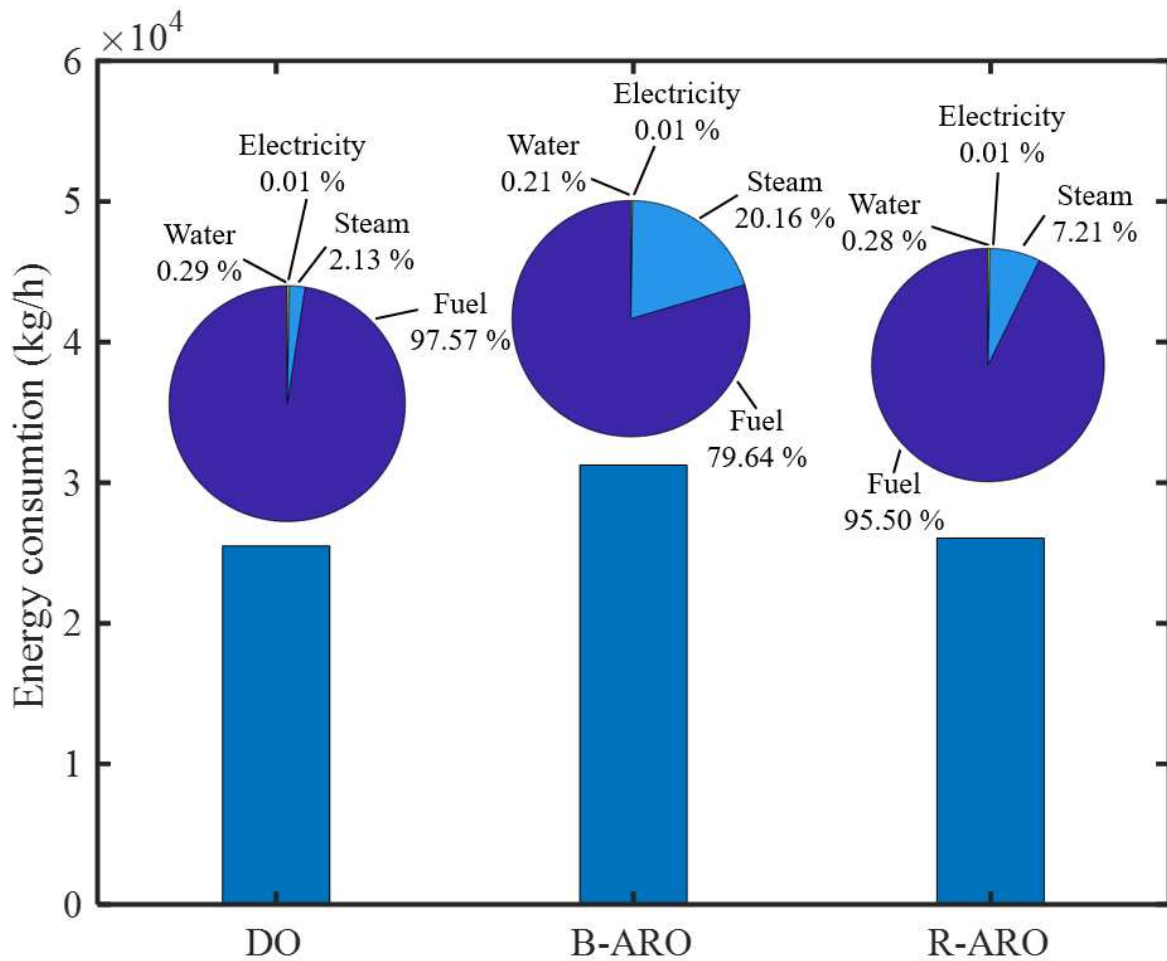


Fig. 7. Comparison of the energy consumption of different optimization methods (DO: Deterministic optimization; B-ARO: Two-stage ARO with a box-based uncertainty set; and R-ARO: Data-driven ARO with RKDE)

The optimal energy system structure and operational conditions under the deterministic and proposed optimization methods are presented in Figs. 8 and 9. The energy system structures after optimization are the same under these two optimization methods. Given that the SS produced in the WHRS can satisfy the steam demand, no boiler was used after optimization. Low process mechanical power users chose electric motors instead of steam turbines. One cooling tower and one water pump were shut down after optimization to reduce the total energy consumption. The steam sent to the letdown valves was greatly reduced to avoid unnecessary energy loss. Compared with the deterministic optimization, more steam was consumed in ST1, ST2, and ST3 under the two-stage adaptive robust optimization method to satisfy the uncertain demands.

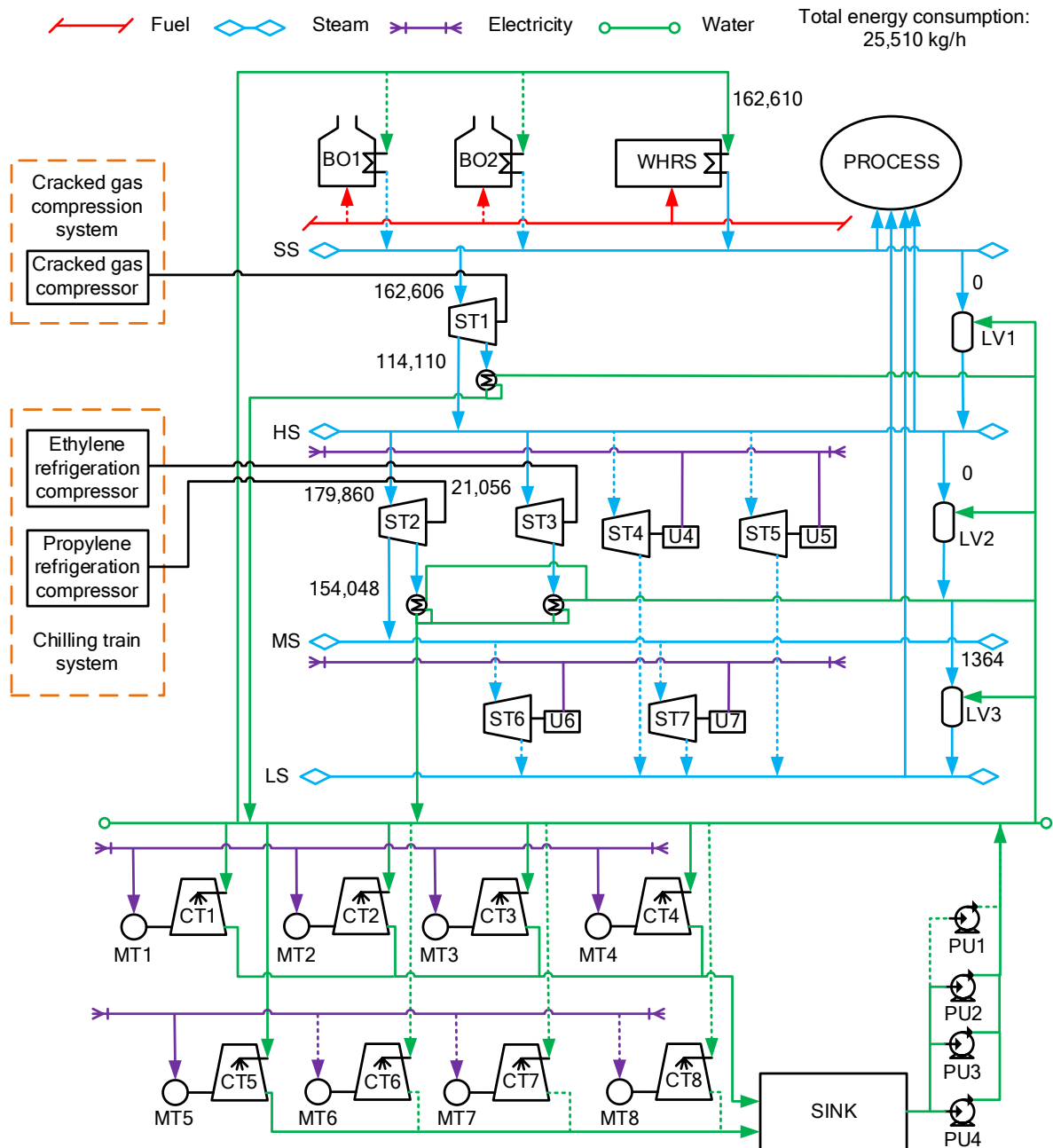


Fig. 8. Optimal structure and operational conditions under deterministic optimization

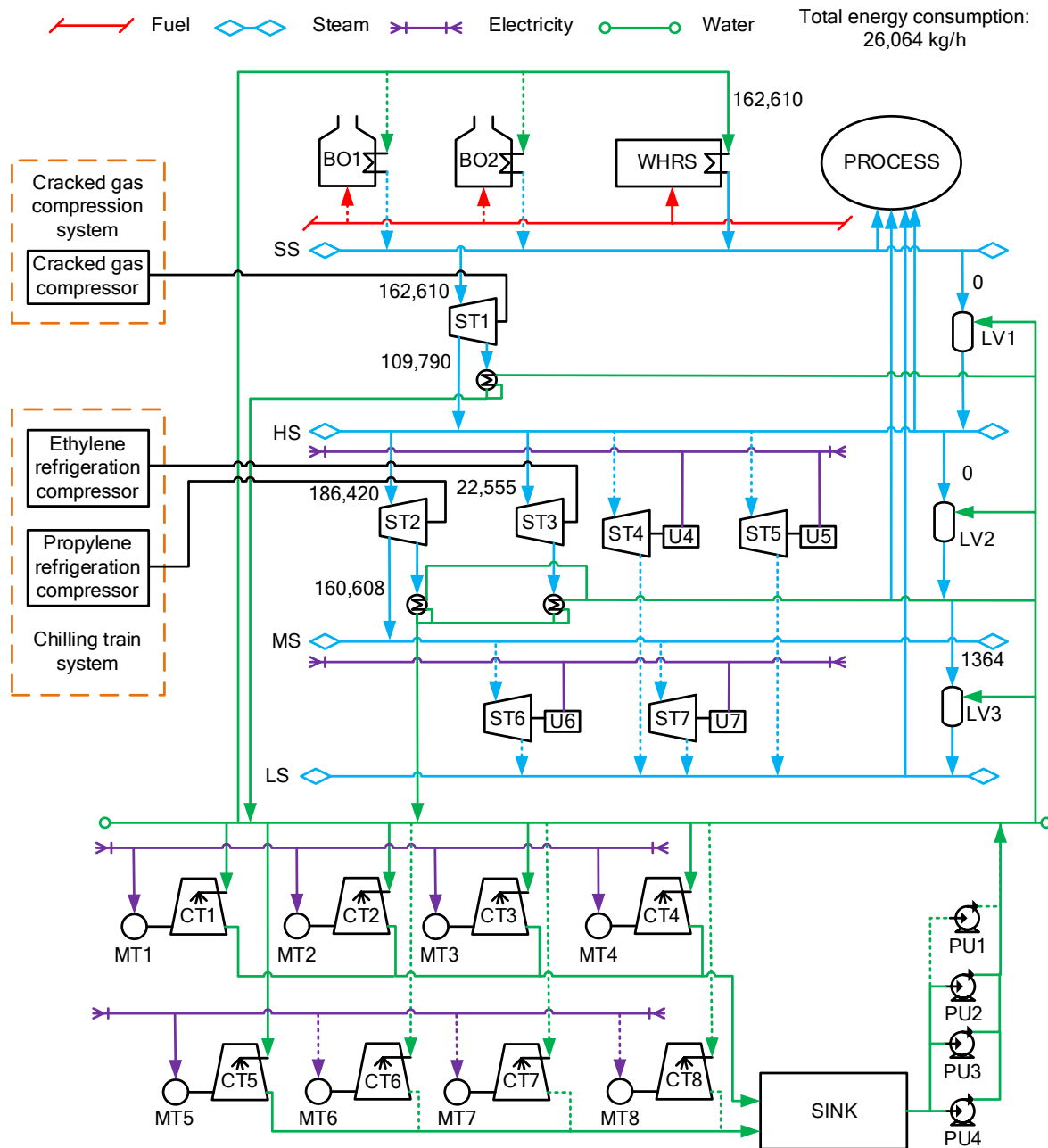


Fig. 9 Optimal structure and operational conditions under data-driven ARO with RKDE

A sensitivity analysis of different uncertainty set parameters is presented in Fig. 10, where α is set to 0.02, 0.05, 0.1, 0.15, and 0.2 and θ is set to 0.05, 0.1, 0.2, 0.4, and 0.8. When θ is fixed to 0.8, the solution under different α ranges from 26,866 kg/h to 29,637 kg/h. The solution increases by 9.66 % on average when α increases from 0.02 to 0.2. The tendency of θ is opposite to that of α . When θ is reduced from 0.8 to 0.05 under fixed α , the solution is improved by 10.13 % on average. Due to the smaller confidence interval corresponding to a larger α , the energy consumption obviously increases along with α under a fixed θ . While θ is the uncertainty budget to control the influence of uncertainty deviations from the center, this parameter only has limited effects on the solution.

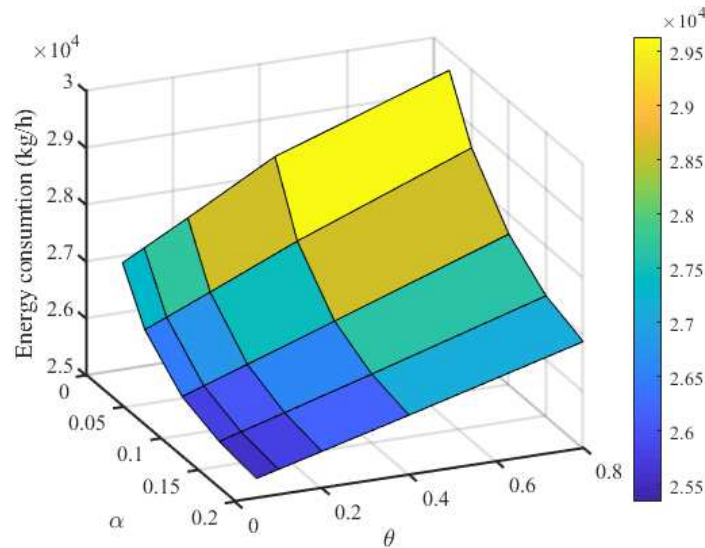


Fig. 10. Optimal energy consumption under different uncertainty set parameters

6. Conclusion

This study addressed the industrial multi-type energy system optimization under demand uncertainty by using a data-driven two-stage adaptive robust optimization model coupling with the power demands of compressors. The uncertain demand deviations from their nominal values were calculated by using accurate Aspen Plus[®] models based on the collected industrial big data for different operation conditions. A machine learning method robust kernel density estimation (RKDE) was adopted to construct the data-driven uncertainty set for capturing the uncertain power demands of compressors. By incorporating the derived uncertainty set, a data-driven adaptive robust energy system optimization model was formulated, where the second-stage decision variables can adjust themselves to the uncertain parameters. The adaptive robust optimization model was rewritten as a single-level mixed-integer non-linear programming problem by affine decision rule. A case study on an industrial ethylene plant multi-type energy system was carried out, and results show that the proposed approach can return an effective and robust solution whose PoR was only 2.18%. The sensitivity analysis shows that the energy consumption under different parameters ranges from 25,350 kg/h to 29,637 kg/h, and the deviation between the worst and best solutions is 16.91%. The parameters of the RKDE-based uncertainty set can be used to adjust the conservatism of the solution. Results of this study can guide the industrial decision-makers in balancing the robustness and optimality.

Notes

The authors declare no competing financial interest.

Acknowledgments

This work was supported by National Key Research and Development Program of China under Grant 2018AAA0101602, International (Regional) Cooperation and Exchange Project (61720106008), National Natural Science Fund for Distinguished Young Scholars (61725301) and National Natural Science Foundation of China (61873092).

Nomenclature

Acronyms

ARO	Adaptive robust optimization
HS	High-pressure steam
LS	Low-pressure steam
MILP	Mixed-integer linear programming
MINLP	Mixed-integer non-linear programming
MS	Medium-pressure steam
PHD	Process historical database
RKDE	Robust kernel density estimation
SC	Steam condensate
SS	Super-high-pressure steam

Sets

bo	Index of boiler set
ct	Index of cooling tower set
i	Index of uncertainty set
lv	Index of letdown valve set
mt	Index of cooling tower electric motor set
mu	Index of standby motor for mechanical power user set
pu	Index of water pump set
st	Index of steam turbine set
stc	Index of steam condenser set

Parameters

α_{bo}, β_{bo}	Parameters in the boiler efficiency regress function
$\varepsilon_{ct}, \phi_{ct}, \varphi_{ct}, \gamma_{ct}$	Parameters in the cooling tower efficiency regress function

ζ_{fuel}	Coefficient of fuel to oil equivalent (kg/kg)
$\zeta_{electricity}$	Coefficient of electricity to oil equivalent (kg/kW)
ζ_{HS}	Coefficient of HS to oil equivalent (kg/kg)
ζ_{MS}	Coefficient of MS to oil equivalent (kg/kg)
ζ_{water}	Coefficient of water to oil equivalent (kg/t)
$CP_{ct,air}^{in}$	Specific heat capacity of inlet air of cooling tower (kg/°C)
$CP_{ct,air}^{out}$	Specific heat capacity of outlet air of cooling tower (kg/°C)
CP_{water}	Specific heat capacity of water (kg/°C)
G_{st}^{user}	Demand of mechanical power user (kW)
H_{bfw}	Enthalpy of fresh water in the boiler (kJ/kg)
H_{SS}	Enthalpy of SS in the boiler (kJ/kg)
$H_{lv,steam}^{in}$	Enthalpy of the inlet steam in the letdown valve (kJ/kg)
$H_{lv,water}^{in}$	Enthalpy of the inlet water in the letdown valve (kJ/kg)
H_{st}^{in}	Enthalpy of the inlet steam in the steam turbine (kJ/kg)
H_{st}^{ext}	Enthalpy of the extraction steam in the steam turbine (kJ/kg)
$H_{lv,steam}^{out}$	Enthalpy of the outlet steam in the letdown valve (kJ/kg)
KA_{stc}	Heat transfer coefficient (kJ · h ⁻¹ · m ⁻² · °C ⁻¹) and heat transfer area (m ²)
$LHV_{bo,fuel}$	Lower heat value of fuel (kJ/kg)
$M_{bo,water}^{max}$	Maximum mass flowrate of water in the boiler (kg/h)
$M_{ct,water}^{max}$	Maximum mass flowrate of water in the cooling tower (kg/h)
r_{water}	Latent heat of vaporization (kJ/kg)

Continuous variables

η_{bo}	Efficiency of boiler
η_{ct}	Cooling tower heat exchange efficiency
δt_{stc}	Terminal temperature difference of steam condensers (°C)
$C_{electricity}$	Electricity consumption (kW)
C_{fuel}	Fuel consumption (kg/h)

C_{HS}	HS consumption (kg/h)
C_{MS}	MS consumption (kg/h)
C_{steam}	Steam consumption (kg/h)
C_{total}	Total energy consumption (kg/h)
C_{water}	Water consumption (kg/h)
G_{st}^{mt}	Power produced by the standby motor for mechanical power user (kW)
G_{st}^{tur}	Power produced by the steam turbine (kW)
H_{st}^{out}	Enthalpy of the exhausting steam in the steam turbine (kJ/kg)
M_{blw}	Mass flowrate of the blowdown (kg/h)
M_{cfw}	Mass flowrate of fresh water (kg/h)
$M_{ct,vapor}$	Mass flowrate of vapor in the cooling tower (kg/h)
M_{st}^{ext}	Mass flowrate of extraction steam (kg/h)
$M_{bo,fuel}^{in}$	Mass flowrate of fuel in the boiler (kg/h)
$M_{bo,water}^{in}$	Mass flowrate of water in the boiler (kg/h)
$M_{lv,steam}^{in}$	Mass flowrate of inlet steam in the letdown valve (kg/h)
M_{steam}^{pro}	Mass flowrate of process steam demand (kg/h)
$M_{lv,steam}^{out}$	Mass flowrate of outlet steam in the letdown valve (kg/h)
M_{st}^{out}	Mass flowrate of the exhausting steam (kg/h)
$M_{stc,water}$	Mass flowrate of water in the steam condenser (kg/h)
P_{stc}^{sat}	Saturated pressure in the steam condenser (kPa)
$Q_{ct,air}$	Heat taken by air in the cooling tower (kJ/h)
$Q_{ct,vapor}$	Heat taken by vapor in the cooling tower (kJ/h)
Q_{water}	Heat taken from water in the cooling tower (kJ/h)
Q_{stc}	Heat transferred in the steam condenser (kJ/h)
$\Delta t_{m,stc}$	Revised logarithm mean temperature difference (°C)
Δt_{stc}	Water temperature difference (°C)
T_{cw}	Temperature of cooling water (°C)
T_{rw}	Temperature of returned water (°C)

$T_{ct,air}^{in}$	Temperature of inlet air in the cooling tower (°C)
$T_{ct,air}^{out}$	Temperature of outlet air in the cooling tower (°C)
T_{steam}^{out}	Temperature of outlet steam of turbine (°C)

Binary Variables

z	Binary variable meaning whether the unit is employed
-----	--

References

- [1] Klemm C, Vennemann P. Modeling and optimization of multi-energy systems in mixed-use districts: A review of existing methods and approaches. *Renew Sustain Energy Rev* 2021; 135:110206. <https://doi.org/10.1016/j.rser.2020.110206>.
- [2] Kueppers M, Paredes Pineda SN, Metzger M, Huber M, Paulus S, Heger HJ, et al. Decarbonization pathways of worldwide energy systems – Definition and modeling of archetypes. *Appl Energy* 2021; 285:116438. <https://doi.org/10.1016/j.apenergy.2021.116438>.
- [3] Shen F, Wang X, Huang L, Ye Z, Qian F. Modeling and Optimization of a Large-Scale Ethylene Plant Energy System with Energy Structure Analysis and Management. *Ind Eng Chem Res* 2019; 58:1686–700. <https://doi.org/10.1021/acs.iecr.8b05247>.
- [4] Shang Z, Kokossis A. A transshipment model for the optimisation of steam levels of total site utility system for multiperiod operation. *Comput Chem Eng* 2004; 28:1673–88. <https://doi.org/10.1016/j.compchemeng.2004.01.010>.
- [5] Luo X, Zhang B, Chen Y, Mo S. Modeling and optimization of a utility system containing multiple extractions steam turbines. *Energy* 2011; 36:3501–12. <https://doi.org/10.1016/j.energy.2011.03.056>.
- [6] Li Z, Zhao L, Du W, Qian F. Modeling and Optimization of the Steam Turbine Network of an Ethylene Plant. *Chin J Chem Eng* 2013; 21:520–8. [https://doi.org/10.1016/S1004-9541\(13\)60530-3](https://doi.org/10.1016/S1004-9541(13)60530-3).
- [7] Zhang X, Yuan J, Xu L, Tian Z, Wang J. Pseudo-online optimization of condenser pressure for the cold-end system with variable speed pumps. *Appl Therm Eng* 2017; 126:339–49. <https://doi.org/10.1016/j.applthermaleng.2017.07.172>.
- [8] Wang C, Liu M, Zhao Y, Qiao Y, Chong D, Yan J. Dynamic modeling and operation optimization

for the cold end system of thermal power plants during transient processes. *Energy* 2018; 145:734–46. <https://doi.org/10.1016/j.energy.2017.12.146>.

- [9] Marti K, Kall P, editors. *Stochastic Programming: Numerical Techniques and Engineering Applications*. vol. 423. Berlin, Heidelberg: Springer Berlin Heidelberg; 1995. <https://doi.org/10.1007/978-3-642-88272-2>.
- [10] Mavromatidis G. Design of distributed energy systems under uncertainty: A two-stage stochastic programming approach. *Appl Energy* 2018; 19.
- [11] Charnes A, Cooper WW. Chance-Constrained Programming. *Manag Sci* 1959; 6:73–9. <https://doi.org/10.1287/mnsc.6.1.73>.
- [12] Shabazbegian V, Ameli H, Ameli MT, Strbac G, Qadrdan M. Co-optimization of resilient gas and electricity networks: a novel possibilistic chance-constrained programming approach. *Appl Energy* 2020:116284. <https://doi.org/10.1016/j.apenergy.2020.116284>.
- [13] Ben-Tal A, Nemirovski A. Robust optimization - methodology and applications. *Math Program* 2002; 92:453–80. <https://doi.org/10.1007/s101070100286>.
- [14] Shen F, Zhao L, Du W, Zhong W, Qian F. Large-scale industrial energy systems optimization under uncertainty: A data-driven robust optimization approach. *Appl Energy* 2020; 259:114199. <https://doi.org/10.1016/j.apenergy.2019.114199>.
- [15] Grossmann IE, Apap RM, Calfa BA, García-Herreros P, Zhang Q. Recent advances in mathematical programming techniques for the optimization of process systems under uncertainty. *Comput Chem Eng* 2016; 91:3–14. <https://doi.org/10.1016/j.compchemeng.2016.03.002>.
- [16] Shang C, Huang X, You F. Data-driven robust optimization based on kernel learning. *Comput Chem Eng* 2017; 106:464–79. <https://doi.org/10.1016/j.compchemeng.2017.07.004>.
- [17] Ning C, You F. Data-driven decision making under uncertainty integrating robust optimization with principal component analysis and kernel smoothing methods. *Comput Chem Eng* 2018; 112:190–210. <https://doi.org/10.1016/j.compchemeng.2018.02.007>.
- [18] Ning C, You F. Data-driven adaptive nested robust optimization: General modeling framework and efficient computational algorithm for decision making under uncertainty. *AIChE J* 2017; 63:3790–817. <https://doi.org/10.1002/aic.15717>.
- [19] Ning C, You F. Optimization under uncertainty in the era of big data and deep learning: When machine learning meets mathematical programming. *Comput Chem Eng* 2019; 125:434–48. <https://doi.org/10.1016/j.compchemeng.2019.03.034>.

- [20] Ben-Tal A, Goryashko A, Guslitzer E, Nemirovski A. Adjustable robust solutions of uncertain linear programs. *Math Program* 2004; 99:351–76. <https://doi.org/10.1007/s10107-003-0454-y>.
- [21] Bertsimas D, Litvinov E, Sun XA, Zhao J, Zheng T. Adaptive Robust Optimization for the Security Constrained Unit Commitment Problem. *IEEE Trans Power Syst* 2013; 28:52–63. <https://doi.org/10.1109/TPWRS.2012.2205021>.
- [22] Lorca Á, Sun XA. Adaptive Robust Optimization With Dynamic Uncertainty Sets for Multi-Period Economic Dispatch Under Significant Wind. *IEEE Trans Power Syst* 2015; 30:1702–13. <https://doi.org/10.1109/TPWRS.2014.2357714>.
- [23] Ning C, You F. Adaptive robust optimization with minimax regret criterion: Multiobjective optimization framework and computational algorithm for planning and scheduling under uncertainty. *Comput Chem Eng* 2018; 108:425–47. <https://doi.org/10.1016/j.compchemeng.2017.09.026>.
- [24] Shi H, You F. A computational framework and solution algorithms for two-stage adaptive robust scheduling of batch manufacturing processes under uncertainty. *AIChE J* 2016; 62:687–703. <https://doi.org/10.1002/aic.15067>.
- [25] Zhao L, Ning C, You F. Operational optimization of industrial steam systems under uncertainty using data-Driven adaptive robust optimization. *AIChE J* 2019; 65:e16500. <https://doi.org/10.1002/aic.16500>.
- [26] Dai X, Wang X, He R, Du W, Zhong W, Zhao L, et al. Data-driven robust optimization for crude oil blending under uncertainty. *Comput Chem Eng* 2020; 136:106595. <https://doi.org/10.1016/j.compchemeng.2019.106595>.
- [27] Zhao L, You F. A data-driven approach for industrial utility systems optimization under uncertainty. *Energy* 2019; 182:559–69. <https://doi.org/10.1016/j.energy.2019.06.086>.
- [28] Shen F, Wang M, Huang L, Qian F. Exergy analysis and multi-objective optimisation for energy system: a case study of a separation process in ethylene manufacturing. *J Ind Eng Chem* 2021; 93:394–406. <https://doi.org/10.1016/j.jiec.2020.10.018>.
- [29] JooSeuk Kim, Scott C. Robust kernel density estimation. 2008 IEEE Int. Conf. Acoust. Speech Signal Process., Las Vegas, NV, USA: IEEE; 2008, p. 3381–4. <https://doi.org/10.1109/ICASSP.2008.4518376>.
- [30] Wang W, Zeng D, Liu J, Niu Y, Cui C. Feasibility analysis of changing turbine load in power plants using continuous condenser pressure adjustment. *Energy* 2014; 64:533–40.

<https://doi.org/10.1016/j.energy.2013.11.001>.

- [31] Ning C, You F. A data-driven multistage adaptive robust optimization framework for planning and scheduling under uncertainty. *AICHE J* 2017; 63:4343–69. <https://doi.org/10.1002/aic.15792>.
- [32] JooSeuk Kim, Scott C. Robust kernel density estimation. 2008 IEEE Int. Conf. Acoust. Speech Signal Process., Las Vegas, NV, USA: IEEE; 2008, p. 3381–4. <https://doi.org/10.1109/ICASSP.2008.4518376>.
- [33] Hastie T, Tibshirani R, Friedman J. *The Elements of Statistical Learning*. New York, NY: Springer New York; 2009. <https://doi.org/10.1007/978-0-387-84858-7>.
- [34] Hampel FR. The Influence Curve and its Role in Robust Estimation. *J Am Stat Assoc* 1974; 69:383–93. <https://doi.org/10.1080/01621459.1974.10482962>.
- [35] Tawarmalani M, Sahinidis NV. A polyhedral branch-and-cut approach to global optimization. *Math Program* 2005; 103:225–49. <https://doi.org/10.1007/s10107-005-0581-8>.
- [36] Bertsimas D, Sim M. The Price of Robustness. *Oper Res* 2004; 52:35–53. <https://doi.org/10.1287/opre.1030.0065>.

Highlight

- (1) Data-driven ARO is firstly applied in industrial multi-type energy systems optimization under uncertainty.
- (2) The data-driven uncertainty set is formed by RKDE based on the industrial big data.
- (3) Deterministic and data-driven ARO are formulated as MINLP problems.
- (4) The effect of the set parameters on the solution is explored.